DOI: 10.13009/EUCASS2019-841

8th European Conference for Aeronautics and Space Sciences (EUCASS), Madrid, Spain, 1-4 July 2019.

SWING – COMPARISON OF PROPELLANT SLOSHING AND EQUIVALENT PEDULUM MODELES WITH A MULTI-COPTER

Olivier Boisneau[I], Eric Bourgeois[I], Jean Desmariaux[I], David-Alexis Handschuh[I], Jérémie HASSIN and Quentin LE JONCOUR[II]

The launchers directorate of CNES has initiated a project to develop a multicopter and to use it as a test-bench for launchers problematic investigations and to test Guidance, Navigation and Flight Control algorithms.
For Flight Control, propellants sloshing are modelled with equivalent pendulums. A device composed by a tank where the liquid can be replaced by its equivalent pendulum was designed. The multicopter with the device was forced to oscillate around one axis to study the oscillations responses of the full system for both configurations.
This paper presents the vehicle and the device. First experimental results are analyzed.

INTRODUCTION

In the last years, multirotor drones have become very common and in easy access. However, for what concerns Guidance, Navigation and Flight Control (GNC), one will find many similarities between Multi-rotors drone and a launcher (free-free conditions, attitude control management, etc., see[1]). Compared to small rockets, they are easier to operate and flights can be chained very quickly.

The launchers directorate of CNES has initiated a small and low-cost internal project (SWING) to develop a multi-rotor drone and to use it has a test bench for launchers problematic investigations and to test Guidance, Navigation and Flight Control (GNC) algorithms.

The first application for this test bench is to study the dynamics of liquid in tanks (propellants sloshing) during the propulsive phase of the flight.

[I] CNES, Launchers Directorate. Contact: olivier.boisneau@cnes.fr
[II] AERACCESS

DOI: 10.13009/EUCASS2019-841

CONTEXT

For Flight Control development and verifications, propellants sloshing in launchers are commonly modelled with equivalent pendulums as described in the NASA SP 106 Abramson's paper[2] or in the new issue of the paper in 2000 by F. T. Dodge[3].

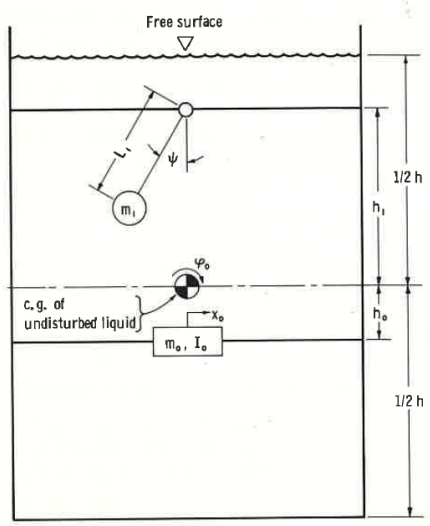

Figure 1 : Dodge slosh Model[2,3]

In this description, propellants sloshing are represented by *n* pendulums representing the *n* first sloshing frequencies. Each pendulum has the mass of liquid moved by the mode. An extra mass is added to represent the mass of liquid not involved by the sloshing and considered as rigidly attached to the tank. The position of this mass is adjusted to keep the center of gravity of the rigidly attached mass and the pendulums equal to the center of gravity of the liquid (when everything is at rest position).

For some simple tank geometries, characteristics of those pendulums can be computed with Dodge equations[2,3]. But, for more complex tank geometries, slosh modes are defined experimentally on ground with tanks on shakers or with CFD computations.

Few experiments have been done in flight for sloshing and most of them are performed during the in-orbit phase[4]. No public results have been found concerning a comparison between actual flight observations of vehicle dynamics submitted to sloshing and the dynamics of the same vehicle with the equivalent pendulum.

Thus, a device was designed for performing this comparison with a multicopter. This device is composed of a tank fixed on a multicopter. The liquid in the tank can be removed and replaced by its equivalent pendulum. To simplify, we consider only the first mode of sloshing and the pendulum has only one degree of freedom.

During the experiment, the multicopter is forced to oscillate around one axis. We compare the oscillations response of the full system for both configurations (i.e. with the liquid and with the pendulum – see Figure 2) at different frequencies and different amplitudes.

Figure 2 : Tests Configurations

DESIGN OF THE DEVICE

Dimensionless number

In his Ph. D dissertation, R. Lebeaud[5] identifies a set of 8 parameters to describe the slosh properties in a cylindrical tank. Those parameters are:

- The level of the liquid: h ;
- The radius of the tank: R ;
- Axial acceleration: a_x ;
- Radial acceleration : a_T ;
- Kinematic viscosity of the liquid: ν ;
- Density of the liquid: ρ ;
- Surface tension: σ ;
- Characteristic time of the perturbation: τ

From this set of parameter, five dimensionless parameters are defined:

- The filling level: $N_1 = \frac{h}{R}$;
- The ratio between the characteristic time of the perturbation and the axial acceleration: $N_2 = \frac{R}{a_x \tau^2}$;
- The ration between the characteristic time of the perturbation and the transverse acceleration: $N_3 = \frac{\tau^2 a_T}{R}$;
- The Bond number which is the ratio between body forces and surface tension: $Bo = \frac{\rho a_x R^2}{\sigma}$;
- The Ohnesorge number which is the ratio between viscous forces and surface tension: $Oh^2 = \frac{\rho \nu^2}{R\sigma}$.

In the case of a heavy launcher, usually:

- Axial and Radial acceleration during propulsive phases are in the range:
  $a_x \in [4;\ 40 m.s^2]$ and $a_T \in [0; 0.5 m.s^{-2}]$
- The maximum level for sloshing is when the frequency of the perturbation is equal to the natural frequencies of sloshing. For a heavy launcher slosh frequencies (at Ig) are in the range of $f_{excitation} \in [0{,}1\ ;\ 0.8\ \text{Hz}]$.

Thus, one has: $N_1 \in [0;\ 3]$, $N_2 \in [0.1; 28.5]$ and $N_3 \in [0; 0.3]$.

Physicals properties of liquid Oxygen and Hydrogen are reported here after. They are compared with water:

	LOx (at 90°K)	LH2 (at 21°K)	Water (at 20°C)
Density (kg.m^{-3})	1 142	70	998
Surface Tension (N.m^{-1})	0.72	0.00182	0.0728
Kinematic Viscosity (m^2.s^{-1})	1.69^{E-7}	1.814^{E-7}	1.007^{E-6}

Table 1 : LOx and LH2 physicals properties

Table 2 compare Bond number and Ohnesorge for a heavy launcher with the case of small 10 cm tank of water embedded in a multicopter:

	Tank Radius (m)	Acc. a_x (m.s^{-2})	Bo	Oh
LOx	5	4	1.59^{E+05}	3.01^{E-06}
		40	1.59^{E+06}	
LH2	5	4	3.85^{E+06}	1.59^{E-05}
		40	3.85^{E+07}	
Water	0.1	4	5.48^{E+02}	3.73^{E-04}
		40	5.48^{E+03}	

Table 2 : Bond number and Ohnesorge number

For liquid oxygen and liquid hydrogen as for water, one has:

- $Oh \ll 1$, thus viscous forces are negligible compare to surface tension;
- $Bo \gg 1$, body forces induced by axial acceleration are predominant versus surface tension.

Then, main conclusions are:

- slosh properties are not affected by the nature of the liquid;
- water can be used in place of liquid oxygen or liquid hydrogen for the device.

Design of the tank

A common shape for a tank in a launcher is a cylinder with spherical cap for the top and the bottom. Slosh frequencies and masses are not described in NASA-SP-106[2,3] for this kind of tank. Indeed, one will find in NASA-SP-106[2,3] all the explanation to compute sloshes properties for a cylinder tank with a flat bottom or for a spherical tank.

Choong-Seok Oh[6] have studied slosh frequencies in a cylinder tank with a spherical bottom of $R=14.26cm$ for N_l in [0.3; 1.75]. Figure 3 presents the comparison between experimental results from Choong-Seok Oh[6] and slosh properties computed from equations of NASA-SP-106[2,3] for a cylinder or a spherical tank. One can conclude that:

- For $N_l \leq 0.66$, experimental results of Choong-Seok Oh[6] can be fitted with the equation of a spherical tank ;
- For $N_l \geq 1.3$, experimental results of Choong-Seok Oh[6] are well described by the equation of a cylinder tank with flat bottom;
- For $0.66 < N_l < 1.3$, none of those equations fit the experimental results.

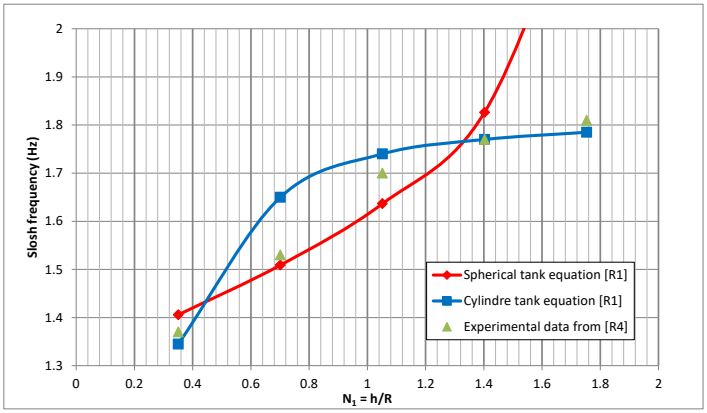

Figure 3 : Comparison of Experimental data from Choong-Seok Oh[6] with slosh equation for a cylinder or a spherical tank

More data are needed to generalize those conclusions to all tanks of this shape but those results have been used as hypothesis to start the design of the tank.

The difficulty was then to find a set of tank radius and level of water able to fit the two following constraints:

1. A mass of liquid lower than *5 kg* to be able to carry out the device on a reasonable multicopter;
2. A frequency in the range of *[0.1, 0.8 Hz]* consistent with 5m diameter launcher sloshing modes under *1g*.

Actually, no set was able to fit both constraints, which led to prioritize the first criteria in order to be able to carry the experiment.

Finally, we retained a configuration with a tank radius R=11.5cm and a level of liquid h=15cm (thus, with a filling level N_l=1.3) that gives a mass of water $m_R = 4.63$kg and a frequency for the first sloshing mode closes to 2Hz.

Design of the equivalent pendulum

For the equivalent pendulum, we chose to test 3 different configurations because we found differences in formulas between the 1966 issue of the NASA-SP-106 and its re-edition in 2000. We also wanted to test a configuration based on the result of an in-house tool (name ASTRAL) that take the real shape of the tank to compute equivalent pendulums.

Six physical parameters are needed to describe the equivalent pendulum. They are shown in the Figure 4. They are:

- L_1: the length of the pendulum;
- l_1: the position of the pendulum relative to the surface of the liquid at rest;
- m_1: the pendulum mass;
- l_0: the position of the rigidly attached mass relative to the surface of the liquid at rest;
- m_0: the rigidly attached mass;
- I_0: the inertia of the rigidly attached mass.

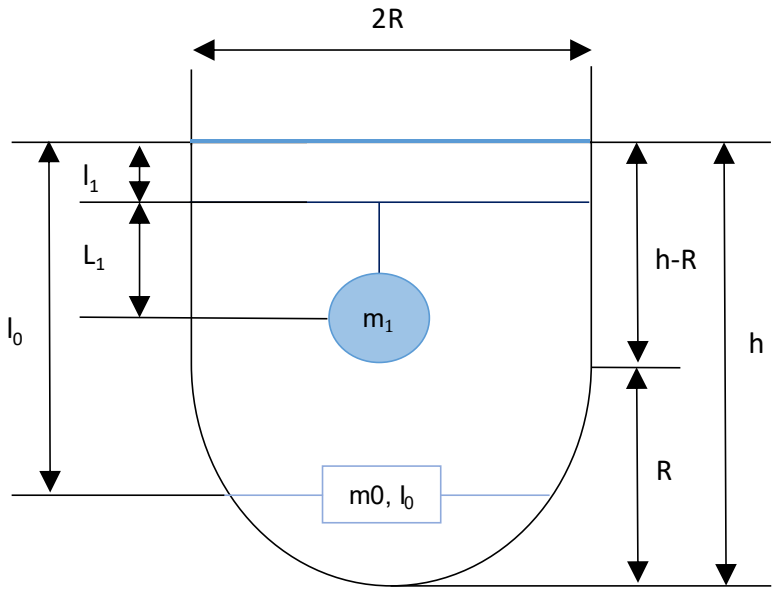

Figure 4 : Equivalent pendulum parameters

Dodge's formulas from the initial version of NASA-SP-106[2] in 1966

In the initial NASA-SP-106[2], Dodge give formulas to compute the characteristics of the equivalent pendulum for the first sloshing mode in case of a cylinder tank with flat bottom. They are recall here after:

- length of the pendulum: $L_1 = \frac{d}{3.68}\coth 3.68\frac{h}{d}$
- Mass of the pendulum: $m_1 = m_T\frac{d}{4.4h}\tanh 3.68\frac{h}{d}$
- Position of the pendulum relative to the surface of the liquid at rest:

$$l_1 = -\frac{d}{7.36}\operatorname{csch} 7.36\frac{h}{d}$$

With $d = 2R$, the diameter of the tank.

Frequency of the first sloshing mode is link to the length of the pendulum and to the acceleration. For an acceleration of $1g = 9.81\ m.s^{-2}$, in our configuration, the frequency is :

$$f = \frac{1}{2\pi}\sqrt{\frac{g}{L_1}} = 1.98\ Hz$$

One can see that length and position of the pendulum are independent from the total mass of liquid m_T. This is not the case for the pendulum mass.

Dodge's formulas have been written for a cylinder tank with flat bottom. In this case, the total mass is:

$$m_T = \rho\pi R^2 h$$

We made the hypothesis that Dodge's formulas are also true for a cylinder tank with spherical cap and we replaced m_T, in the formulas, with the real mass of our device. For a cylinder tank with spherical cap, the volume of liquid is the sum of the hemisphere part (with a radius R) and the cylinder part (whose height is: $h - R$). Thus, the mass of liquid in the tank is:

$$m_T = \rho\frac{2\pi R^3}{3} + \rho\pi R^2(h - R)$$

The rigidly attached mass is computed to keep the center of gravity at the same position as the center of gravity of the liquid at rest. Thus:

$$m_0 = m_T - m_1$$

The center of gravity for the cylinder tank with spherical cap is the barycenter of the cylinder part $X_{G_{cyl}}$ and the hemisphere part $X_{G_{sph}}$. Where:

$$X_{G_{sph}} = (h - R) + \frac{\rho}{m_{sph}}\int_{r=0}^{R}\int_{\alpha=0}^{2\pi}\int_{\beta=0}^{\frac{\pi}{2}} r^3\cos\beta\sin\beta\, dr\, d\alpha\, d\beta = (h - R) + \frac{\rho}{m_{sph}}\frac{\pi R^4}{4}$$

Thus:

$$X_{G_{sph}} = h - \frac{5}{8}R$$

The barycenter of the cylinder part is:

$$X_{G_{cyl}} = \frac{h - R}{2}$$

Thus:

$$X_G = \frac{m_{cyl}X_{G_{cyl}} + m_{sph}X_{G_{sph}}}{m_T} = \frac{3h^2 - 2hR + R^2}{6h - 2R}$$

And, finally:

$$l_0 = \frac{m_T}{m_0}X_G - \frac{m_1}{m_0}(l_1 + L_1)$$

For the inertia, Dodge give this equality:

$$I_0 + m_0 l_0^2 + m_1(l_1 + L_1)^2 = I_{cyl}^G + m_T\left(\frac{h}{2}\right)^2 - \frac{m_T d^2}{8}\left[1.995 - \frac{d}{h}\left(\frac{1.07cosh\left(3.68\frac{h}{d}\right) - 1.07}{sinh\left(3.68\frac{h}{d}\right)}\right)\right]$$

With:

$$I_{cyl}^G = m_T\left[\frac{h^2}{12} + \frac{R^2}{4}\right]$$

The left part represents the inertia of the system: pendulum + rigidly attached mass.

I_{cyl}^G is the inertia of the liquid computed at its center of gravity. Thus, the two first term of the right part of the equality are the inertia of the liquid computed at the its surface.

The first part of this equation expresses the equality between the inertia of the system composed of the pendulum and the rigidly attached mass and the inertia of the liquid when everything is at rest. Origin of the last term is not explained in the NASA SP-106.

As the numerical value of I_0 is low compare to the inertia of our device, we made the assumption that, for the tank with spherical cap, the inertia of the liquid is the same as for a tank with flat bottom.

Dodge's formulas from the re-edition of the NASA-SP-106[3] in 2000

For the new issue of the NASA SP-106[3] in 2000, for the case of a cylinder tank with flat bottom, formulas for the first sloshing mode have been generalized to any sloshing mode. Thus, characteristics of the equivalent pendulum for the nth sloshing mode are:

- The length of the pendulum : $L_n = \frac{d}{2\xi_n \tanh(2\xi_n h/d)}$;
- The pendulum mass : $m_n = m_T \left[\frac{d \tanh(2\xi_n h/d)}{\xi_n(\xi_n^2 - 1)h}\right]$;
- Position of the pendulum from the center of gravity of the tank:

$$H_n = \frac{h}{2} - \frac{d}{2\xi_n}\left[\tanh(\xi_n h/d) - \frac{1}{\sinh(2\xi_n h/d)}\right]$$

Formulas for the length and the mass of the equivalent pendulum of the first sloshing mode are the same as in the first issue of NASA SP-106 since $\xi_1 = 1.841$.

This is not the case for the position of the pendulum where one has:

$$l_n = \frac{h}{2} - H_n = \frac{d}{2\xi_n}\left[\tanh(\xi_n h/d) - \frac{1}{\sinh(2\xi_n h/d)}\right]$$

Like in the first issue of NASA SP-106, the rigidly attached mass is computed to keep the center of gravity at the same position as the one of the liquid at rest. Thus:

$$m_0 = m_T - \sum_{n=1}^{\infty} m_n$$

And, its position from the surface of the liquid at rest is:

$$l_0 = \frac{m_T}{m_0} X_G - \frac{1}{m_0} \sum_{n=1}^{\infty} m_n (l_n + L_n)$$

For our device, we kept only the first sloshing mode (n=1). Thus, formulas for m_0, l_0, L_1 and m_1 are the same as for Dodge 1966.

For the position of the pendulum, we have:

$$l_1 = \frac{d}{2\xi_1}\left[\tanh(\xi_1 h/d) - \frac{1}{\sinh(2\xi_1 h/d)}\right]$$

As the position of the fixed mass l_0 is link to l_1, this evolution impact also the numerical value of l_0.

In the new issue of the NASA SP-106[3], Dodge considers that the moment of inertia is only a fraction of the moment of inertia of the "frozen liquid". Thus, he presents the evolution of the ratio between the system pendulums + rigidly attached mass and the inertia of the "frozen liquid" in function of the liquid depth ratio h/d (see Figure 5).

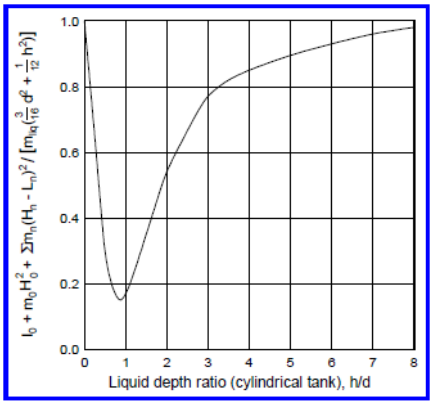

Figure 5 : Ratio of model to frozen liquid moment of inertia for a cylindrical tank[3]

In our device, $h/d = 0.65$, thus :

$$I_0 + m_0 H_0^2 + \sum m_n (H_n - L_n)^2 \approx 0.2\, I_{cyl}^G$$

We kept the first sloshing mode, thus, for a cylinder tank with flat bottom:

$$I_0 = 0.2 I_{cyl}^G - m_0 H_0^2 - m_1 (H_1 - L_1)^2$$

As the numerical value of I_0 is low compare to the inertia of our device, we made the assumption that, for the tank with spherical cap, the inertia of the liquid is the same as in the case of a tank with flat bottom.

Astral compute sloshing

We wanted also to test a configuration based on the result of our in-house finite element software (Astral) that compute sloshing modes properties for any tank with axis-symmetric shape.

The software formulation is based on the fluid-structure interaction methods developed by Morand and al[7].

The tool computes up to 25 sloshing modes but, for our configuration, after the 7th mode, masses of pendulums are lower than 1gr. Pendulums characteristics are presented here after:

N° Mode	Frequency (Hz)	Length of the pendulum L_n (m)	Pendulum Mass m_n (kg)	Position of the Pendulum from the Surface of the liquid l_n (m)
1	1.95	0.065	2.028	0.092
2	3.41	0.021	0.062	0.039
3	4.33	0.013	0.015	0.026
4	5.09	0.010	0.006	0.019
5	5.77	0.007	0.003	0.015
6	6.40	0.006	0.002	0.012
7	7.01	0.005	0.001	0.010

Table 3 : ASTRAL Equivalent pendulums properties

The position, the mass and the inertia of the rigidly attached mass are also given by the software taking into account the 25 sloshing modes.

For our device, we take only values of the first mode for the pendulum and we didn't add any correction in the property of the rigidly attached mass for the truncation. It leads to a reduction of 2.4% of the global mass of the system pendulum + rigidly attached mass compare to the liquid mass. This reduction is only 11gr and it should be compare to the 8kg of the device.

Synthesis:

Characteristics of the pendulum and the rigidly attached mass are summarized here after for the three configurations of our device:

	Dodge 1966	**Dodge 2000**	**ASTRAL**
L_1	6.4 cm	6.4 cm	6.5 cm
m_1	2.13 kg	2.13 kg	2.03 kg
l_1	-0.5 mm	-4.1 cm	2.7 cm
Freq	1.98 Hz	1.98 Hz	1.95 Hz
m_0	2.50 kg	2.50 kg	2.49 kg
l_0	5.58 cm	9.0 cm	3.35 cm
I_0	$3.4e^{-2}kg.m^2$	$8.2e^{-4}kg.m^2$	$4.3e^{-5}kg.m^2$

Table 4 : Parameters of the pendulum and of the rigidly attached mass for the three configurations

The main differences are on position of the pendulum and on position of the rigidly attached mass. The difference is up to 6.8cm between ASTRAL results and Dodge 2000 formula for the position of the pendulum.

Because of those differences, we have adapted the conception of the device to be able to adjust all the parameters of the pendulum and the rigidly attached mass for the three configurations of equivalent pendulum.

Conception of the device

Figure 6 present two possible configurations of the device. The first one is for the test with water. The second is with the equivalent pendulum.

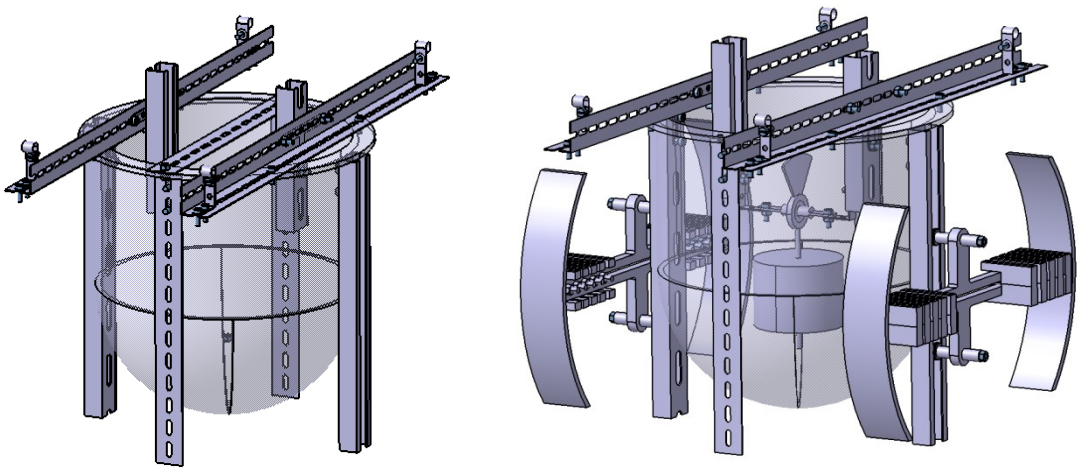

(a) (b)

Figure 6 : The two device configurations

The pendulum is composed in three part (see Figure 7):

- a cylindrical mass in steel;
- a threaded shaft that permit to adjust the length of the pendulum;
- an additional part that made the pivot connection with the rotation axis. The upper shape of this part has been designed to measure the angle of the pendulum.

The pivot connection is ensured by a cylindrical roller bearing.

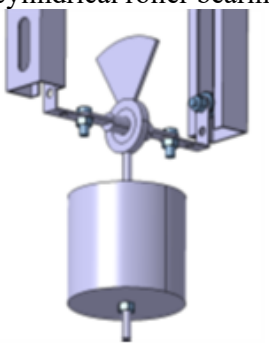

Figure 7 : Diagram of the pendulum

Figure 8 present the final result of the device. One can see its main parts:

- the tank in Plexiglas;
- the structure on the top of the tank that ensure the mechanical connection with the multicopter;
- the two aluminum sections that came inside the tank. They are used to attach the axis of rotation of the pendulum;

- the two aluminum sections outside of the tank. They are used to fix the rigidly attached mass;
- The pendulum;
- The extra leads outside of the tank represent the rigidly attached mass of the Dodge's model.

The tank and the aluminum sections are always present on the device to kept the same mass and the same inertia in all configurations.

The rigidly attached mass of the Dodge's model has been adapted from the theoretical model because it would have block the rotation of the pendulum. It has been split in two parts which have been placed outside of the tank and from either side to respect the balance of the device. Their masses are $\frac{m_0}{2}$ and their shapes have been design to fit the inertia $\frac{I_0}{2}$. Some flyweights can be added to adjust the value of the inertia for the 3 configurations with pendulum.

Figure 8 : The device in its configuration with pendulum

Positions of the pendulum rotation axis and the two rigidly attached masses can be adjusted for each of the three configurations with pendulum.

DESIGN OF THE MULTICOPTER

The device filled with water is about *8 kg*. For raising this device, a heavy multicopter is needed. We chose to build an octocopter with a frame of *1.3 m* large and with *18 inch* propellers.

All the electronic devices and most parts of the octocopter are off-the-shelf. Some structural parts have been manufactured by AERACESS.

Figure 9 : Octocopter without device

For the control of the octocopter, we use an autopilot hardware based on the Pixhawk open source controller. We selected the firmware autopilot developed by the open source project ArduPilot[Erreur ! Signet non défini.].

The autopilot hardware Pixhawk has his own accelerometer and gyro. It is also equipped with a magnetometer and a barometer. The octocopter has also an external GNSS chip which another magnetometer. For the altitude, we added a Lidar.

The vehicle is controlled either by a radio command either by the autopilot. For automatic flights, it can be ordered by a ground control station (a simple PC) with a bi-directional radio frequency link. It is powered by two batteries type lipo 6S with a capacity of 10 000 mAh.

The octocopter is equipped with two cameras (Figure 10).

- The first one observes the top of the tank thanks to a windows left in the structure on the top of the tank.
- The second one has a view of the side of the tank. It is attached to the same structure as the rigidly attached masse.

Both camera supports are fixed with dampers to the octocopter to reduce vibration. Camera are autonomous and have their own memory card.

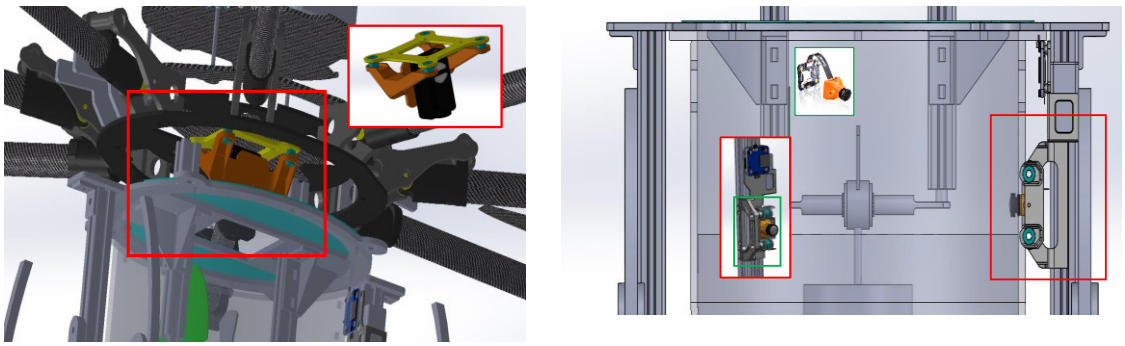

Figure 10 : Position of cameras

Flight control specific design

For the experiment on sloshing, the octocopter has to perform oscillations around one of its axes (roll only here). To have regular oscillations, the roll command is computed by the autopilot himself. For this, we implement a new automatic flight mode in the firmware.

This new mode used the different control loops already developed for the others modes and available as generic functions.

For the experimental protocol, we chose to have a first phase with the vehicle controlled by a pilot with the radio command. After a good health check of the quadcopter, the pilot places the vehicle to a desired altitude and position.

The frequency and the amplitude of the oscillation are sent to the quadcopter by the ground control station. Then, the pilot starts the automatic sequence of oscillations.

This sequence is divided in 3 steps:

- A waiting phase to put the multicopter in a hover position with a fixe altitude command and attitude command set to zero.
- The oscillation phase. During this phase, the autopilot generates a sinusoid command for the roll angle. An additional control loop is active to maintain the quadcopter to a stable altitude.
- The sequence ends with a waiting phase identic to the first step. The aim of this phase is to return to the hover position before leaving the automatic flight.

The altitude control loop has been added after the first tests because altitude tended to evolve during the oscillation phase.

The structure of the pilot is illustrated here after. One will recognize the 3 steps on the roll command:

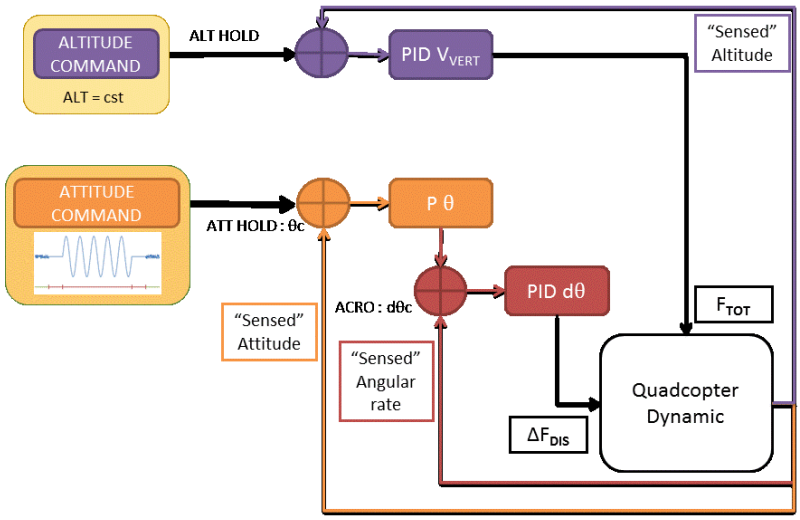

Figure 11 : View of the controller structure for the automatic experimental mode

FIRST RESULTS ANALYSIS

We have already tests in flight 2 configurations of the device:

- The first one with water;
- The second with the equivalent pendulum base on Dodge's formulas from edition 1966 of the NASA SP-106.

Because the octocopter is too big to flight indoor, each test has been performed outside. To limit the wind influence on the result, we tried to select days with moderate wind to flight. We also placed the vehicle in front of the wind during the automatic sequences of oscillations. In function of the intensity of the wind, the drift of the octocopter was more or less important but always perpendicular to its oscillations. Between two tests, the pilot had to bring back the vehicle to his point of departure.

Tests were performed between 2 or 3 meters high to benefit from the LIDAR precision to control the altitude.

Despite the presence of the 2 batteries, flights could never last more than 5 minutes.

Experiment with water

Figure 12 present the octocopter in flight with the configuration of the device with water.

Figure 12 : Octocopter in the air with the device in configuration with water

On Figure 13, a view from the camera at the side of the tank is presented. One can see the 3 dimensional shape of the wave. Some post-treatments are needed now to analyze those movies to measure the free surface and to find sloshing properties.

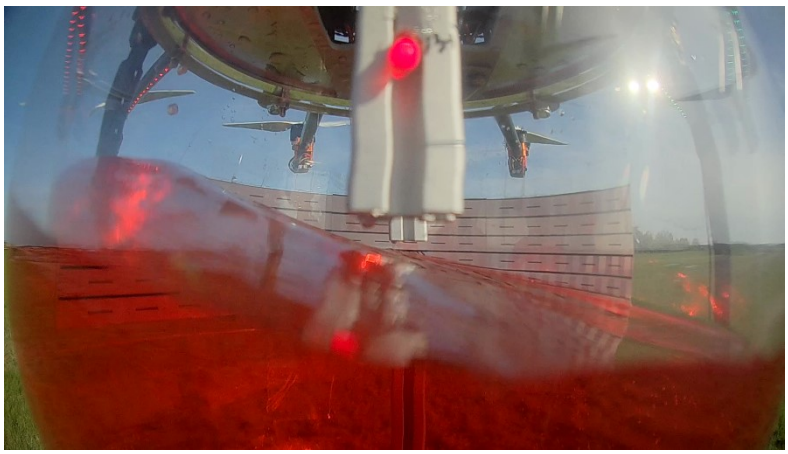

Figure 13 : Side view of the tank during the experiment

Some examples of the response of the vehicle to the forced oscillation are presented on Figure 14 for 4 different excitation frequencies.
In total, 12 different frequencies have been tested for 3 different levels of amplitude.

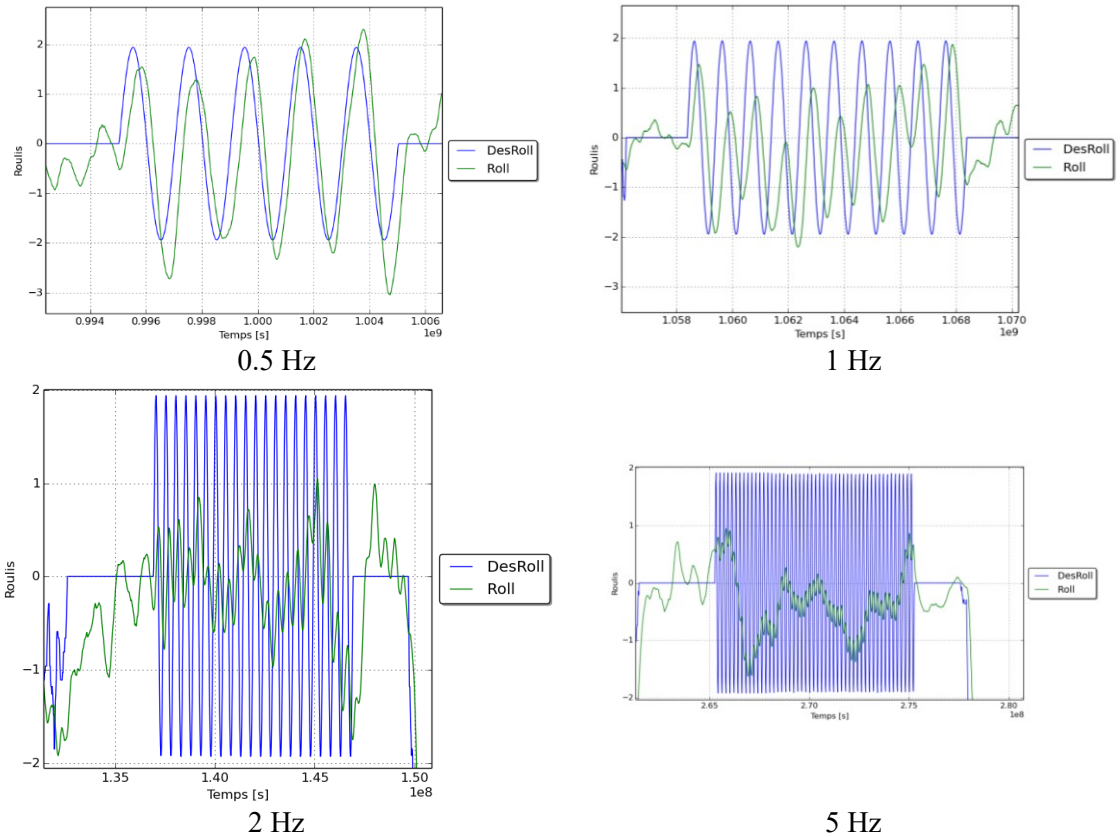

Figure 14 : Response to forced-oscillations for the configuration with water

Experiment with the equivalent pendulum base on Dodge's formulas from 1966 edition of NASA SP-106

Figure 15 present the octocopter in flight with the configuration of the device with the equivalent pendulum.

Figure 15 : Octocopter in the air with the pendulum configuration

On Figure 16, views from the camera at the top and at the side of the tank are presented during the oscillation of the octocopter. Some post-treatments are needed now to analyze those movies to measure the angle of the pendulum in function of the time.

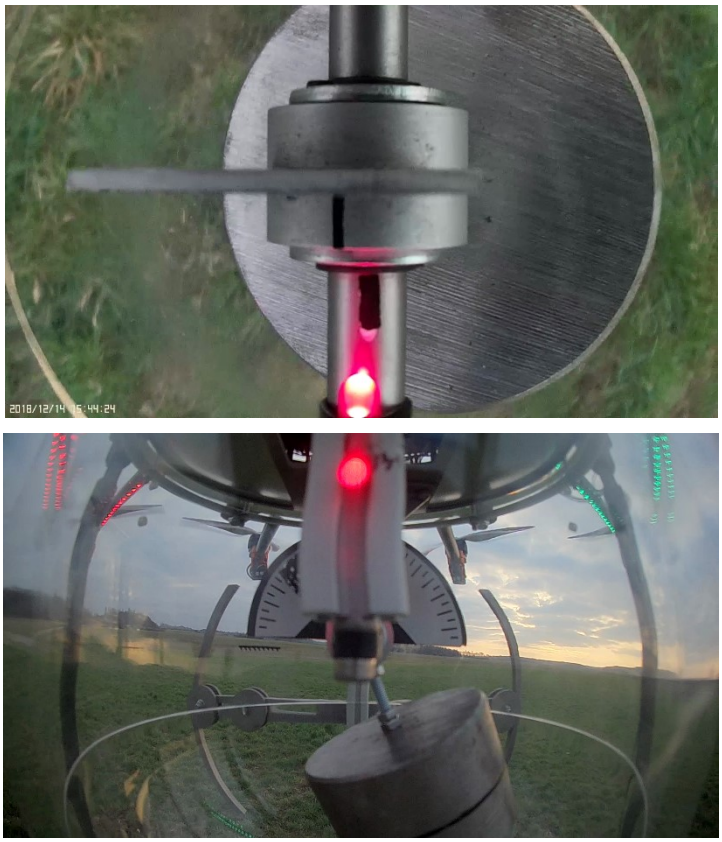

Figure 16 : Top and side views of the pendulum during the experiment

Some examples of the response of the vehicle to the forced oscillation are presented on Figure 17 for 4 different excitation frequencies.

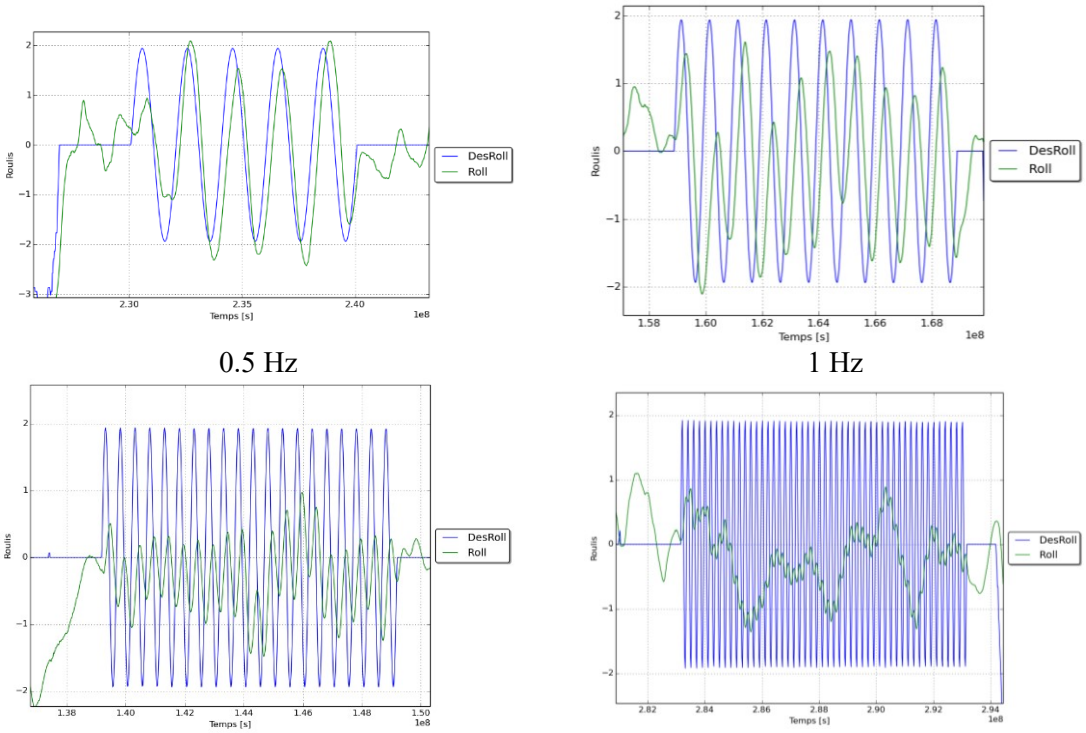

Figure 17 : Response to forced-oscillations for the configuration with the equivalent pendulum

Response to forced-oscillations

Twelve frequencies from *0.2 Hz* to *10 Hz* have been tested for three different amplitudes. For each case, the oscillations phase lasted 10s.

For each test, oscillation amplitude of the vehicle attitude response (B) has been compared with the oscillation amplitude of the command (A). The gain was defined as:

$$gain = 20\, log10\left(\frac{B}{A}\right) \quad (1)$$

Results are plotted in Figure 20 in a Bode diagram.

Some filtering has been used to find the vehicle attitude response (B) because the roll attitude signal is not exploitable like this. For each signal, a Fast Fourier Transformation has been performed to determine a cut-off frequency (Figure 18). From the FFT results, every frequency bellow the cut-off frequency has been remove to the original signal. The results are plotted in Figure 19. One will find also in Figure 19 the filtered roll signal and the command roll signal used to compute the gain.

DOI: 10.13009/EUCASS2019-841

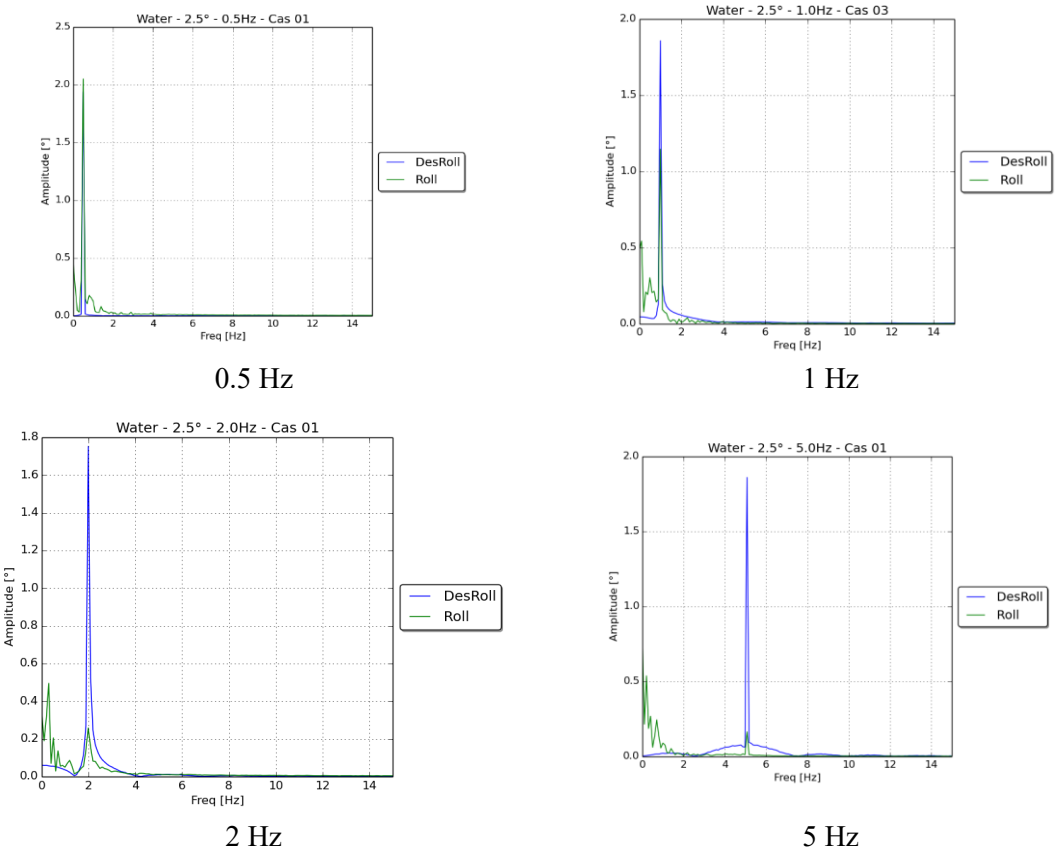

0.5 Hz 1 Hz

2 Hz 5 Hz

Figure 18 : FFT of the roll and roll command signals

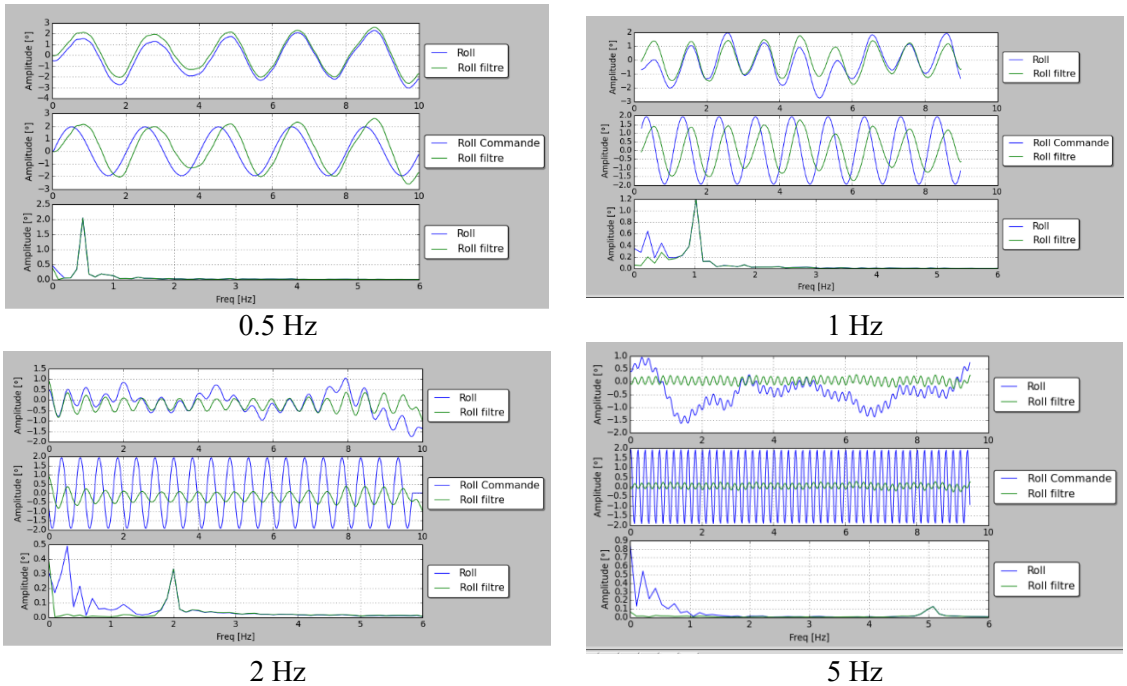

0.5 Hz 1 Hz

2 Hz 5 Hz

Figure 19 : Filtering and signal reconstruction

Globally, in Figure 20, for frequencies between 0.5Hz and 2.5 Hz, results are similar for the configuration with water and for the one with the equivalent pendulum from Dodge's formula.

For both cases the cutoff frequency seems to near 0.7Hz or 0.8Hz. However, the overall shapes of curves are different especially for frequencies above 5Hz. The order of the transfer function could be different.

Those results will have to be confirmed with the analysis of data from others amplitude of oscillation and with those of the 2 others configurations of pendulum.

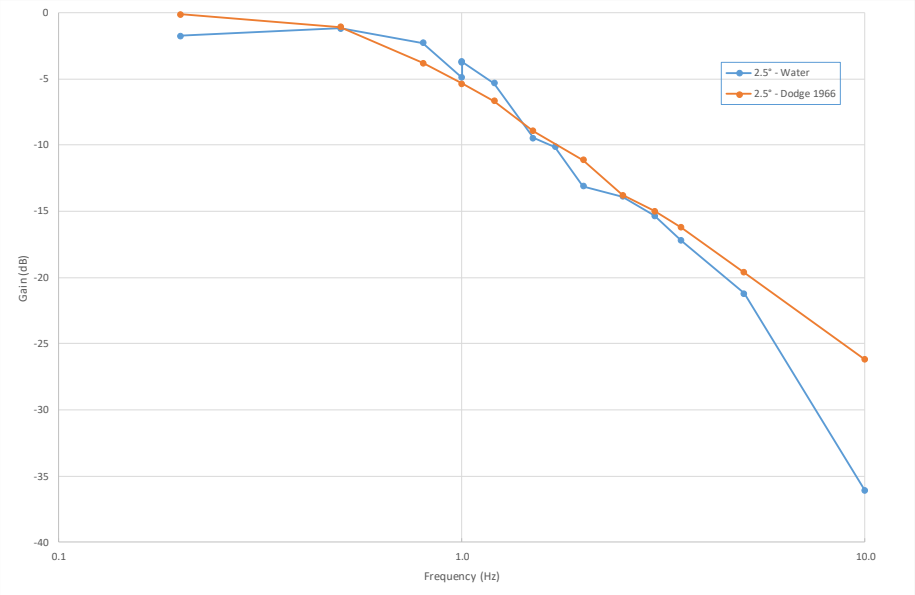

Figure 20 : Bode diagram of the first results

CONCLUSION

CNES launchers directorate has initiated an internal project to develop a multi-rotor drone and to use it as a test bench for launchers problematic investigations. The first application for this test bench is to study propellants sloshing.

A device has been designed that allow to study the response to forced-oscillations of a vehicle composed by an octocopter and a tank with fill with water. The water can be replaced in the device by its equivalent pendulum as models described by Dodge in NASA SP-106 articles.

Three different configurations are possible for the equivalent pendulum.

The configuration with the tank fill with water and the one with the equivalent pendulum base on the edition 1966 of the NASA SP-106 have been already test in flight.

Analysis of the results are one going. A comparison of transfer functions of the two configurations is presented. Results show that, for frequencies between 0.5Hz and 2.5 Hz, gains are similar for the configuration with water and for the one with the equivalent pendulum but that the overall shapes of curves are different especially for frequencies above 5Hz.

Those results have to be confirmed with additional verifications and also with the results of the 2 configurations of pendulum not tested already.

REFERENCES

[1] O. Boisneau, E. Bourgeois, J. Desmariaux, D.-A. Handschuh, A. Espinosa, J. Franc, "*Use of Multicopter for launchers problematic investigations*", AAS 17-223, 27th AAS/AIAA Space Flight Mechanics Meeting, San Antonio, 2017
[2] ABRAMSON, "*The dynamic Behavior of Liquids in Moving Containers*", NASA SP-106*,* 1966
[3] F. T. Dodge, "*The New Dynamic Behavior of Liquids in Moving Containers*", Southwest Research Inst., 2000
[4] M. Eswaran and Ujjwal K. Saha, "*Sloshing of liquids in partially filled tanks – a review of experimental investigations*", OCEAN SYSTEMS ENGINEERING 1 (2), 131-155, 211
[5] Royon-Lebeaud, 2005, "*Ballottement des liquides dans les réservoirs cylindriques soumis à une oscillation harmonique: régimes d'onde non-linéaire et brisure.*", *Grenoble: archives-ouvertes.fr*, 2005
[6] Choong-Seok Oh, Byung-Chan Sun, Yong-Kyu Park, Woong-Rae Roh, "Sloshing Analysis Using Ground Experimental Apparatus", *International Conference on Control, Automation and Systems,* Seoul, 2008
[7] Morand, H., J.P., Ohayon, R., "Fluid-Structure Interaction", John Wiley & Sons, 1995